

## 研究成果の刊行に関する一覧表

### 【書籍】

著者氏名	論文タイトル名	書籍全体の編集者名	書籍名	出版社名	出版地	出版年	ページ
Onishi H, Nambu A, Kimura T, Nagata Y.	Stereotactic radiotherapy for non-small cell lung cancer-computed tomography.	Hayat	Cancer Imaging	Lippincott	USA	2007	215-229
大西洋	非小細胞肺癌の従来型放射線治療	渋谷均ら	エビデンス放射線治療	中外医学社	日本	2007	141-147
染谷正則 晴山雅人	放射線急性反応	渋谷 均 晴山雅人 平岡真寛	エビデンス放射線治療	中外医学社	東京	2007	7-13

### 【雑誌】

発表者氏名	論文タイトル名	発表誌名	巻号	ページ	出版年
Norihisa Y, <u>Nagata Y</u> , Takayama K, Matsuo Y, Sakamoto T, Sakamoto M, Mizowaki T, Yano S, <u>Hiraoka M</u> .	Stereotactic body radiotherapy for oligometastatic lung tumor.	Int J Radiat Oncol Biol Phys			In press
Zhu S, Mizowaki T, Norihisa Y, Takayama K, <u>Nagata Y</u> , <u>Hiraoka M</u> .	Comparisons of the impact of systematic uncertainties in patient setup and prostate motion on doses to the target among different plans for definitive external-beam radiotherapy for prostate cancer.	Int J Clin Oncol.	13(1)	54-61	2008
Matsuo Y., Takayama K., <u>Nagata Y.</u> , Kunieda E., Tateoka K., Ishizuka N., Mizowaki T., Norihisa Y., Sakamoto M., Narita Y., Ishikura S., <u>Hiraoka M</u> .	Interinstitutional variations in planning for stereotactic body radiation therapy for lung cancer.	Int J Radiat Oncol Biol Phys	68(2)	416-25	2007

<u>Nagata Y.</u> , Matsuo Y., Takayama K., Norihisa Y., Mizowaki T., Mitsumori M., Shibuya K., Yano S., Narita Y., <u>Hiraoka M.</u>	Current status of stereotactic body radiotherapy for lung cancer.	Int J Clin Oncol.	12(1)	3-7	2007
Matsuo Y., <u>Nagata Y.</u> , Mizowaki T., Takayama K., Sakamoto T., Sakamoto M., Norihisa Y., <u>Hiraoka M.</u>	Evaluation of mass-like consolidation after stereotactic body radiation therapy for lung tumors.	Int J Clin Oncol	12(5)	356-62.	2007
Yamamoto T., Mizowaki T., Miyabe Y., Takegawa H., Narita Y., Yano S., <u>Nagata Y.</u> , Teshima T., <u>Hiraoka M.</u>	An integrated Monte Carlo dosimetric verification system for radiotherapy treatment planning.	Phys Med Biol	52(7)	1991-2008	2007
<u>Hiraoka M.</u> , Matsuo Y., <u>Nagata Y.</u>	Stereotactic body radiation therapy (SBRT) for early-stage lung cancer	Cancer Radiother	11(1-2)	32-5	2007
<u>Hiraoka M.</u> , <u>Ishikura S.</u>	A Japan clinical oncology group trial for stereotactic body radiation therapy of non-small cell lung cancer.	J Thorac Oncol	2 (7 Suppl 3)	S115-117	2007
Yuichiro Kamino, Sadao Miura, <u>Masaki Kokubo</u> , Ichiro Yamashita, Etsuro Hirai, <u>Masahiro Hiraoka</u> , Junzo Ishikawa	Development of an ultrasmall C-band linear accelerator guide for a four-dimensional image-guided radiotherapy system with a gimbaled x-ray head.	Med Phys	34	1797-808	2007
Yuichiro Kamino, Kazuhiro Tsukuda, <u>Masaki Kokubo</u> , Sadao Miura, Etsuro Hirai, <u>Masahiro Hiraoka</u> , Junzo Ishikawa	Development of a new concept automatic frequency controller for an ultrasmall C-band linear accelerator guide.	Med Phys.	34	3243-8	2007

Imura M, ..Shirato H, et al.	Histopathologic Consideration of Fiducial Gold Markers Inserted for Real-Time Tumor-Tracking Radiotherapy Against Lung Cancer.	Int J Radiat Oncol Biol Phys.			In press
Murphy MJ, ...Shirato H, et al.	The management of imaging dose during image-guided radiotherapy: report of the AAPM Task Group 75.	Med Phys	34(10)	4041-63	2007
Onimaru R, ..Shirato H.	Steep Dose-Response Relationship for Stage I Non-Small-Cell Lung Cancer using Hypofractionated High-Dose Irradiation by Real-Time Tumor-Tracking Radiotherapy.	Int J Radiat Oncol Biol Phys	70(2)	374-81	2008
Someya M, Sakata K, Matsumoto Y, Tauchi H, Narimatsu H, <u>Hareyama M</u>	Association of DNA-PK activity and radiation-induced NBS1 foci formation in lymphocytes with clinical malignancy in breast cancer patients	Oncology Reports	18(4)	873-878	2007
Sakata K, Someya M, Omatsu M, Asanuma H, Hasegawa T, <u>Hareyama M</u>	The enhanced expression of the matrix metalloproteinase 9 in nasal NK/T-cell lymphoma	BioMed Central Cancer	7(1)	229	2007
舘岡邦彦、大内敦、長瀬大輝、佐藤崇史、中田健生、清水目一成、 <u>晴山雅人</u>	MLCファントムを用いた三次元放射線治療計画システムにおけるNon-dosimetricQA	日本放射線腫瘍学会誌			2008 (印刷中)

小塚拓洋、五味光太郎、熊田まどか、利安隆史、尾上剛士、鶴貝雄一郎、根本景子、大川綾子、能勢隆之、小口正彦、 <u>山下孝</u>	肺癌への定位照射	臨床放射線			2008年 1月号
Koto M, Takai Y, Ogawa Y, Matsushita H, Takeda K, Takahashi C, Britton KR, Jingu K, Takai K, Mitsuya M, Nemoto K, Yamada S.	A phase II study on stereotactic body radiotherapy for stage I non-small cell lung cancer.	Radiotherapy and Oncology	85	429-434	2007
Jingu K, Nemoto K, Kaneta T, Oikawa M, Ogawa Y, Ariga H, Takeda K, Sakayauchi T, Fujimoto K, Narazaki K, Takai Y, Nakata E, Fukuda H, Takahashi S, Yamada S.	Temporal change in brain natriuretic Peptide after radiotherapy for thoracic esophageal cancer	.Int J Radiat Oncol Biol Phys	1;69(5)	1417-23	2007
Onishi H, Shirato H, Nagata Y, Hiraoka M, Fujino M, Gomi K, Niibe Y, Karasawa K, Hayakawa K, Takai Y, Kimura T, Takeda A, Ouchi A, Hareyama M, Kokubo M, Hara R, Itami J, Yamada K, Araki T.	Hypofractionated stereotactic radiotherapy (HypoFXSRT) for stage I non-small cell lung cancer: updated results of 257 patients in a Japanese multi-institutional study.	J Thorac Oncol	7	S94-100	2007
大西洋、萬利乃寛、斉藤亮、荒屋正幸、青木真一、栗山健吾、小宮山貴史、荒木力.	I期非小細胞肺癌に対する定位放射線治療の現状	山梨肺癌研究会誌	20	41-45	2007
大西洋、萬利乃寛、青木真一、荒屋正幸、斉藤亮、佐野尚樹、芦沢和成、荒木力.	胸腹2点式簡易呼吸インジケータ(アブチェス)とバイオフィードバック効果を応用した自己呼吸停止下照射—4D(動物)の3D(静止)化のメリット	臨床放射線	53	411-416	2008
T. Kawase E. Kunieda H.M. Deloar, S. Seki, A. Sugawara T.	Experimental stereotactic irradiation of normal rabbit lung. Analysis by computed	Radiat Med	25(9)	453-61	2007

Tsunoo, E.N. Ogawa A. Ishizaka K. Kameyama A. Takeda, A. Kubo	tomography of radiation injury and their histopathological features				
E. Kunieda H.M. Deloar S. Takagi K. Sato T. Kawase H. Saitoh K. Saito O. Sato G. Sorell, A. Kubo	Interface software for DOSXYZnrc Monte Carlo dose evaluation on a commercial radiation treatment planning system	Radiat Med	25(6)	309-14	2007
茂松直之 奥洋平 国枝悦夫 久保敦司 高見博	甲状腺疾患に対する放射線 外照射	日本臨牀	65(11)	2053-60	2007
S. Seki E. Kunieda A. Takeda, T. Nagaoka, H.M. Deloar, T. K awase, J. Fukada, O. Kawaguchi, M. Uem atsu, A. Kubo	Differences in the definition of internal target volumes using slow CT alone or in combination with thinslice CT under breath-holding conditions during the planning of stereotactic radiotherapy for lung cancer	Radiotherapy and Oncology	85(3)	443-9	2007
E. Kunieda N. Kishitan i H.M. Deloar T. Fujis aki T. Kawase S. Seki Y. Oku A. Ku bo	Variation of dose distribution of stereotactic radiotherapy for small-volume lung tumo rs under different respiratory conditions (in printing)	Physica Medica			2008
A. Takeda, E. Kunied a, T. Takeda, M. T anaka, N. Sanuki, H. Fujii, N. Shigemat su, A. Kubo	Possible misinterpretation o f demarcated solid patterns of radiation fibrosis on CT scans as tumor recurrence in patients receiving hypofractionated stereotactic radiotherapy for lung cancer	Int J Radiat Oncol Biol Phys	70(4)	1057-65	2008

<p>A. Takeda, M. Takahashi, <u>E. Kunieda</u>, T. Takeda, N. Sanuki, Y. Koike, K. Atsukawa, T. Ohashi, H. Saito, N. Shigematsu, <u>A. Kubo</u></p>	<p>Hypofractionated stereotactic radiotherapy with and without transarterial chemoembolization for small hepatocellular carcinoma not eligible for other ablation therapies: Preliminary results for efficacy and toxicity.</p>	<p>Hepato Res</p>	<p>38(1)</p>	<p>60-69</p>	<p>2008</p>
<p>唐澤克之他</p>	<p>Body frameを用いた体幹部定位放射線治療時の呼吸性移とsetup error</p>	<p>臨床放射線</p>	<p>53</p>	<p>396-402</p>	<p>2008</p>
<p>川島礼子, 中尾恵, <u>小久保雅樹</u>, 湊小太郎</p>	<p>放射線動体追尾照射のための肺腫瘍の変位推定及び可視化方法</p>	<p>電気情報通信学会論文誌</p>	<p>印刷中</p>		

## 研究成果の刊行物・別刷

ORIGINAL ARTICLE

SuYu Zhu · Takashi Mizowaki · Yoshiki Norihisa  
Kenji Takayama · Yasushi Nagata · Masahiro Hiraoka

## Comparisons of the impact of systematic uncertainties in patient setup and prostate motion on doses to the target among different plans for definitive external-beam radiotherapy for prostate cancer

Received: May 25, 2007 / Accepted: September 11, 2007

### Abstract

**Background.** We aimed to compare the impact of systematic uncertainties in patient setup and prostate motion on three different external-beam radiotherapy protocols for prostate cancer.

**Methods.** To simulate possible near-maximum systematic errors, the isocenter position was shifted to eight points with  $\pm 1.65SD$  of the integrated uncertainty value along each axis that was expected to include 5%–95% of the total systematic uncertainties in each direction. Five cases were analyzed for the three plans: an old three-dimensional conformal radiotherapy (3D-CRT) protocol (four-field plus dynamic arc), a new 3D-CRT protocol (dynamic arc), and an intensity-modulated radiotherapy (IMRT) protocol, respectively.

**Results.** The averaged percentage volume covered by more than 95% of the prescription dose (V95) of the clinical target volume (CTV) for the original plans was 100% for all protocols. After simulating the errors, V95 of the CTV for IMRT cases was maintained at 100%. On the other hand, these values for the new and old 3D-CRT protocols were 93.1% and 63.2%, respectively. The values for the percentage prescription dose received by at least 95% volume (D95) of the CTV for the original plans were 100%, 98.4%, and 97.6% for the IMRT, new 3D-CRT, and old 3D-CRT plans, respectively. However, when the effects of the systematic errors were taken into consideration, the net decreases in the D95 values were 0.3%, 4.3%, and 8.1%, respectively.

**Conclusion.** The current IMRT protocol is considered to successfully compensate for systematic uncertainties. In contrast, the multi-leaf collimator (MLC) margins set for the old 3D-CRT protocol were not enough to ensure the

actual delivery of the prescription dose to the CTV. Therefore, it is very important to include these issues in the plan design in the interpretation of clinical outcomes.

**Key words** Systematic uncertainties · Dynamic-arc 3D-CRT · IMRT · Prostate cancer

### Introduction

Geometrical uncertainties in radiotherapy can cause differences between the planned and the actually delivered dose distribution. The uncertainties mainly consist of setup deviation and internal organ motion. Both uncertainties can be separated into random and systematic components.

Setup error and organ motion in external-beam radiotherapy for prostate cancer have been widely investigated using megavoltage film or an electronic portal image device (EPID),<sup>1–3</sup> sequential computed tomography (CT) scans,<sup>4–9</sup> implanted radiopaque markers,<sup>3,10–12</sup> and a B-Mode Acquisition and Targeting System (BAT).<sup>13,14</sup> With better understanding of these uncertainties, the margin added to the clinical target volume (CTV) to create the planning target volume (PTV) is gradually reduced in conformation therapy to reduce the irradiated dose and volume to the organs at risk and to increase the dose to the CTV. However, a PTV margin that is too small will result in geometrical errors at some or even all treatment fractions. It has therefore become increasingly important to quantify and verify whether the applied margins can account for the uncertainties. Among the components of errors, random errors mainly result in blurring the dose distribution.<sup>15,16</sup> This blurring due to the random errors tends to have a relatively small impact on doses to the target and normal structures.<sup>15</sup> On the other hand, systematic errors have a much larger potential to cause significant underdosing or overdosing to both the target and normal structures.<sup>8,15,17</sup>

Therefore, the present study was designed to compare the effect of systematic components of setup errors and prostate motion on prostate dose coverage among three

S.Y. Zhu · T. Mizowaki (✉) · Y. Norihisa · K. Takayama · Y. Nagata · M. Hiraoka  
Department of Radiation Oncology and Image-applied Therapy,  
Graduate School of Medicine, Kyoto University, 54 Shogoin-  
Kawahara-cho, Sakyo, Kyoto 606-8507, Japan  
Tel. + 81-75-751-3762; Fax + 81-75-771-9749  
e-mail: mizo@kuhp.kyoto-u.ac.jp



**Table 1.** Summary of the three definitive radiotherapy protocols

Protocols	Fields	PTV margins (mm)	MLC and jaw margins (mm)	Setup	Dose (Gy)	Dose prescription
Old 3D-CRT	MLC- Shaped box	Not created	Superior: 12 Inferior: 12 Lateral: 7	Supine without fixation	46	Isocenter
	Dynamic arcs	Not created	Superior: 12 Inferior: 12 Lateral: 7		24	Isocenter
New 3D-CRT	Dynamic arcs	9 (6, Posterior)	Superior: 8 Inferior: 8 Lateral: 3	Supine without fixation	74	Isocenter
IMRT	215° 280° 0° 75° 145°	9 (6, Posterior)	Dynamic MLC, automatic defined: 7–9mm	Prone with hip fixation	74	D95 of the PTV = 95% (>90%)

PTV, planning target volume; MLC, multi-leaf collimator

definitive external-beam radiotherapy plans for localized prostate cancer, and hence to verify whether the margins set for the three protocols could account for those uncertainties.

## Patients, materials, and methods

### Description of the three definitive radiotherapy protocols

Since 1998, three definitive radiotherapy protocols have been applied to the treatment of localized prostate cancer at our institute. They are the old three-dimensional conformal radiotherapy (3D-CRT), new 3D-CRT and intensity-modulated radiotherapy (IMRT) protocols, respectively. Details of each planning protocol have already been reported.<sup>18</sup> Briefly, in the old 3D-CRT protocol, a planning target volume (PTV) was not created. A multileaf collimator (MLC) with a leaf width of 1 cm was directly fitted to the clinical target volume (CTV), which is the prostate, with margins. Forty-six Gy in 23 fractions was given, using the four-field box technique with MLC conformation to the CTV, followed by an additional 24 Gy in 12 fractions with the dynamic-arc conformal technique. In the four-field irradiation, MLC or jaw edges were placed directly on the CTV with margins of 12 mm in superior/inferior directions and 7 mm in the remaining directions based on the beam's eye view of each field. If a part of the posterior rectal wall was included in the lateral opposing fields, the MLC positions were manually adjusted to completely shield the posterior wall from the irradiated area by the bilateral fields. In the dynamic-arc conformal radiotherapy, two lateral arcs with 100° of rotation (from 36° to 136°, and from 226° to 326°) were used with dynamic conformal fitting of MLCs to the CTV with a 7-mm margin. In the new 3D-CRT and IMRT protocols, PTV was created by adding a 9-mm margin to the CTV, except for the posterior rectal-prostate interface, where a 6-mm margin was applied. For the new 3D-CRT protocol, two lateral dynamic arcs with 100° of rotation (from 36° to 136° and from 226° to 326°) were used by dynamic conformal fitting of MLCs to the PTV, in which a 3-mm margin was generally placed from the edge of the PTV to the tips of the MLCs. With respect to the superior

and inferior directions, jaws were fitted with an 8-mm margin to the PTV to ensure 95% dose at the edge of the PTV. For the IMRT protocol, inverse optimization was used to achieve the goal that the percentage prescription dose received by at least 95% volume (D95) of the PTV should generally exceed 95% (at least 90%). The old and new 3D-CRT techniques are performed with the patients in the supine position without any fixation, while IMRT is applied with the patients immobilized in the prone position, using thermoplastic shells fixed to a rigid pelvic board Hip Fix (MedTec, Inc, Orange City, IA, USA) extending from the mid-thigh to the upper third of the leg and with the feet being put on a cushion support. Details of the three protocols are summarized in Table 1.

### Institutional measured uncertainties

From March 2001 to March 2002, a study was conducted to measure setup errors and prostate motion using serial computed tomography (CT) verification scans. Ten patients in the supine position, without fixation devices, and eight patients in the prone position, fixed with a set of thermoplastic shells, were enrolled in the study. Three CT verification scans were performed at 2-week intervals for the whole course of radiotherapy for each patient. CT scans were conducted with the same conditions as the simulation scans; that is, empty rectum and moderately dilated bladder (0.5–1.0 h after micturition). The three serial CT scan images were registered to the simulation CT scan images using the same Digital Imaging and Communications in Medicine (DICOM) coordinates. The prostate was contoured and the center was reconstructed. Four reference points on the pelvic bony structure (two on the innermost edge of the femoral head, one on the anterior-superior edge of the coccyx, and one on the posterior-superior edge of the pubic symphysis) were chosen to calculate the relative position of the prostate along three axial directions. Compared with the relative prostate position on the simulation CT images, the systematic and random prostate motions were calculated. The systematic displacement was taken to be the difference between the prostate position in the planning scan and the mean position as calculated from the three treatment scans, and the random displacements were calculated as the devia-

**Table 2.** Institutional data of systematic uncertainties and the integration used for simulations

	1 SD of systematic setup error		1 SD of systematic prostate motion		1 SD of integrated systematic error ( $\Sigma\delta^2 = IM^2 + SM^2$ )		Simulating value 1.65SD (5%–95% CI)	
	Prone	Supine	Prone	Supine	Prone	Supine	Prone	Supine
LR (mm)	1.6	3.0	0.8	0.9	1.8	3.1	3.0	5.1
AP (mm)	1.6	3.4	2.1	3.7	2.6	5.0	4.3	8.3
CC (mm)	3.1	3.2	3.1	1.7	4.4	3.6	7.3	5.9

LR, Left-right; AP, anterior-posterior; CC, cranial-caudal;  $\delta$ , total margin; IM, internal margin; SM, setup margin; CI, confidence interval

tion of the prostate position in each treatment scan from the mean position. Thus, one systematic and three random displacements were calculated for each patient. Regarding the whole study cohort, the SD for the systematic error was assessed as the SD of the ten patients in the supine position or the eight patients in the prone position. The SD for the random error was taken as the SD of 30 random displacements in the supine position or 24 in the prone position for the ten or eight patients, respectively. The differences between simulation and treatment CT coordinate positions of the center of the four pelvic bony reference points along three axes were, accordingly, calculated as the axial setup errors; the SD values of systematic errors are displayed in Table 2.

Isocenter shifting model simulating systematic setup errors and prostate motion

*Integration of the systematic errors of the setup and internal prostate motion*

The International Commission on Radiation Units and Measurements (ICRU) report 62 discussed several scenarios about how to composite the internal margin (IM) with the setup margin (SM). The report recommended creating a “global” safety margin to be adopted by means of the quadrature formalism ( $\Sigma\delta^2 = IM^2 + SM^2$ ) in a quantitative approach.<sup>19</sup> According to the recommendation, we integrated setup errors and organ motions because the simple linear addition of two kinds of error would lead to an excessively large integrated systematic error. The calculated values of integrated systematic errors along the three axes are indicated in Table 2, for the supine and prone positions separately.

*Representative shifting value of 1.65 SD along each of the three Cartesian directions*

We assume that the prostate motions and setup errors can each be described by three orthogonal independent Gaussian (normal) distributions. This is a reasonable assumption, because several groups have proved that the data are nor-

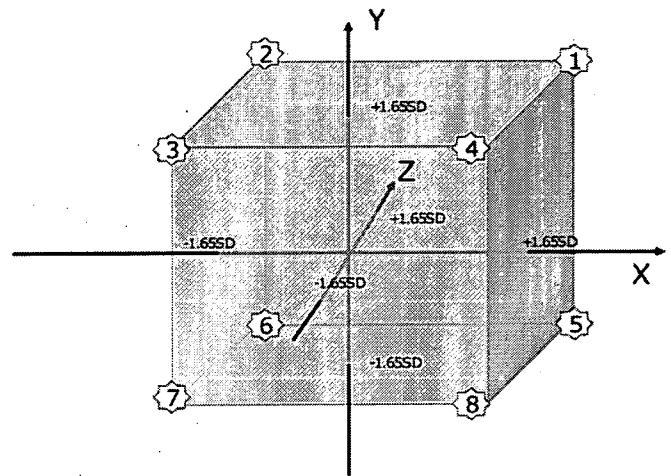


**Fig. 1.** Isocenter shifting model:  $\pm 1.65$  SD was first chosen as the coordinate for axial check points (three pairs). Based on the six axial check points, eight vector combination points were created. The eight corner points were the worst-case scenario within a  $\pm 1.65$  SD axial value

mally distributed.<sup>4,7,10,20</sup> In this case, the calculated integrated systematic uncertainties should also be in normal distribution. Therefore, 90% (5% to 95%) of the systematic uncertainties are included within  $\pm 1.65$  SD. This is because, if we consider a patient group as a whole, the mean value of the systematic errors would be very close to zero, as indicated in our institutional results. Therefore, in this study, we chose 1.65SD of the integrated systematic uncertainties on each of the three axes, which was expected to cover 90% of the systematic isocenter shifts in each direction.

*Simulating the impacts of the systematic errors on the dose distribution*

To simulate the impacts of possible large systematic errors on the dose distribution, we shifted the isocenter to the eight points with  $\pm 1.65$  SD value on each axis (vector combination points; Fig. 1).

The isocenter shifting was conducted on five IMRT plans in the prone position with hip fixation, and on five new 3D-CRT plans in the supine position without fixation, and on

the old 3D-CRT plans created using the new 3D-CRT patients' contoured images strictly complying with the protocols. To further compare the new 3D-CRT protocol with the IMRT protocol, the five new 3D-CRT plans were created based on the respective CT data set for IMRT plans in the prone position with fixation devices complying with the planning protocol accordingly. The same magnitude of systematic uncertainties in the prone position with the fixation device was applied to simulate shifting the isocenter. All the created plans were checked and were approved by our department board. Shifted plans were created and dose distributions were recalculated. In total, 160 shifted plans were created and statistical data were collected and analyzed.

#### Analyses based on dose volume histogram (DVH) data

With the Eclipse treatment planning system (Varian Medical Systems, Inc., Palo Alto, CA, USA), the DVHs of the PTV and the CTV (prostate) were calculated for the original plans and the total shifted plan. The total shifted plan was defined as the plan with the averaged dose distribution of the eight shifted plans for each case. Therefore, the total shifted plan was considered to be the plan reflecting the averaged effect of the simulated systematic uncertainties. For the PTV and CTV, the percentage volume covered by more than 95% of the prescription dose (V95) and the percentage prescription dose received by at least 95% volume (D95) were calculated. In addition, minimal, maximal, and mean percent doses were collected for analyses. The dose conformity to the PTV was calculated using the conformity index (CI) equation advocated by Van't Riet et al.<sup>21</sup> The CI is defined as the product of the fraction of the PTV receiving at least 95% of the prescription dose and the ratio of the volume of the PTV receiving at least 95% of the prescription dose to the body volume receiving at least 95% of the prescription dose, which is indicated by the following equation:

$$\text{Conformity index (CI)} = \frac{\text{VPTV95\%}}{\text{VPTV}} * \frac{\text{VPTV95\%}}{\text{Vt}}$$

Here, VPTV95% is the PTV volume covered by 95% of the prescription dose, VPTV is the volume of the PTV, and Vt is the body volume covered by 95% of the prescription

dose. Therefore, the CI accounts for both any normal tissue volume receiving at least 95% of the prescription dose and for any volume of the PTV receiving less than 95% of the prescription dose. For the new and old 3D-CRT plans, because the same patients' images and systematic uncertainties for simulations of isocenter shifting were applied, comparisons of the DVHs for the same PTV and CTV were made. New 3D-CRT plans created on the CT data sets in the prone position were also compared to the corresponding IMRT plans with respect to the DVH indexes. The DVHs for the shifted plan for each case were calculated using a summed plan function with the same weight assigned to each single shift. The mean DVHs both for the original and shifted plans for each protocol were calculated by averaging their corresponding percentage volume at the same incremental dose steps. The *P* value was calculated by the two-tailed paired Student's *t*-test.

## Results

Table 3 and Table 4 show the planning results of the PTV and CTV for five cases using the three respective protocols. The V95 and D95 values of the CTV for the three protocols were almost comparable (*P* > 0.05) and the differences in the other indexes among the three protocols were also small. However, when the same PTV definition as for the new 3D-CRT and IMRT protocols was applied to the old 3D-CRT protocol, the V95, D95, mean dose, and CI for the old 3D-CRT cases were greatly inferior to those for the cases with the other two protocols (*P* < 0.001), indicating

**Table 4.** RTP results for CTV with the three protocols

	IMRT (mean ± SD)	New 3D-CRT (mean ± SD)	Old 3D-CRT (mean ± SD)
V95 (%)	100 ± 0	100 ± 0	99.9 ± 0.1
D95 (%)	100 ± 0.9	98.4 ± 0.7	97.6 ± 0.6
Minimum dose (%)	98.1 ± 1.2	97 ± 0.6	95.3 ± 1.1
Maximum dose (%)	108.3 ± 1.8	102.6 ± 0.4	101.2 ± 0.5
Mean dose (%)	103.7 ± 0.7	100.7 ± 0.7	99.6 ± 0.3

V95, Percent target volume receiving 95% of the prescription dose or higher; D95, percent prescription dose covering 95% of the target volume

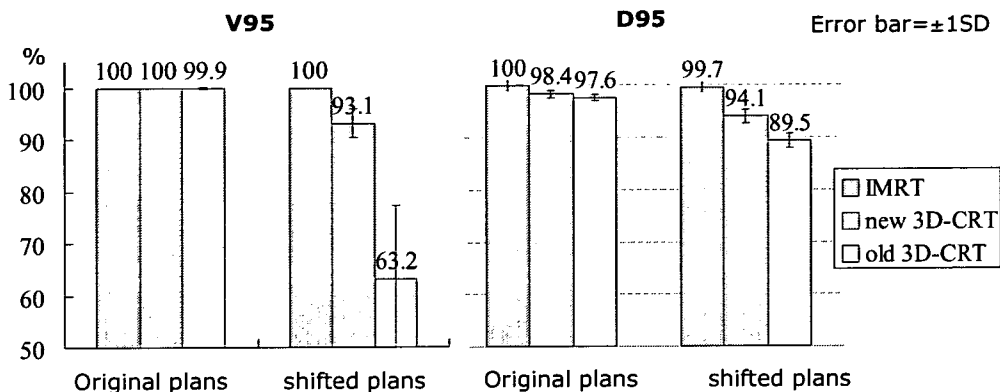
**Table 3.** RTP results for PTV with the three protocols

	IMRT (mean ± SD)	New 3D-CRT (mean ± SD)	Old 3D-CRT (mean ± SD)
V95 (%)	99 ± 0.5	93.9 ± 0.9	59.6 ± 6.8
D95 (%)	97 ± 0.5	94.5 ± 0.3	82.9 ± 1.5
Minimum dose (%)	87.7 ± 4.8	87.5 ± 0.7	60 ± 3.3
Maximum dose (%)	108.5 ± 1.8	102.6 ± 0.4	101.3 ± 0.5
Mean dose (%)	102.3 ± 0.7	99.5 ± 0.3	94.9 ± 1
Conformity index	0.88 (0.87–0.89)	0.76 (0.72–0.78)	0.60 (0.52–0.65)

V95, Percent target volume receiving 95% of the prescription dose or higher; D95, percent prescription dose covering 95% of the target volume; conformity index =  $\frac{\text{V}_{\text{PTV95\%}}}{\text{V}_{\text{PTV}}} * \frac{\text{V}_{\text{PTV95\%}}}{\text{Vt}}$ <sup>21</sup>

For conformity index: mean (range)

**Fig. 2.** Mean percent target volume receiving 95% of the prescription dose or higher (V95) and percent prescription dose covering 95% of the target volume (D95) for dose volume histogram (DVH) of the clinical target volume (CTV) of the three protocols before and after taking systematic uncertainties into consideration. Error bar,  $\pm 1$  SD. MRT, modulated radiotherapy; 3D-CRT, three-dimensional conformal radiotherapy



the original MLC margins set for this protocol are insufficient if the dose evaluation is based on the current PTV concept. The CI for the IMRT plans was the highest among the three protocols, which indicates the dose distributions in the IMRT plans conform best to the PTV compared to those in the new and old 3D-CRT plans.

Figure 2 indicates the V95 and D95 of the CTV for the original plans and the simulated isocenter-shifted plans. The V95s for all three protocols were excellent and reached 100% of the prescribed dose, while D95 values were also 97% or higher for all protocols. On the other hand, although the averaged V95 for total shifted IMRT plans was maintained at 100%, those for the new 3D-CRT and old 3D-CRT plans decreased to 93.1% and 63.2%, respectively. The decreasing rate of the V95 values for the old 3D-CRT cases was most evident compared with those for the other two protocol's cases. The same trend as for V95 was observed with respect to D95, although the magnitudes of the deterioration after simulating the systematic uncertainties in the old 3D-CRT cases were relatively smaller than those for the V95. The net decrease for IMRT cases was minimum (0.3%), while that for the old 3D-CRT cases was the biggest (8.1%) among the three protocols.

Figure 3 indicates the mean DVHs of the CTV for the original and total shifted plans of the three protocols. For the IMRT protocol, the two curves almost coincided with each other. Compared with the original new 3D-CRT plans, definitive insufficient dose coverage was observed with respect to the total shifted plans. Again here, the worsening of the CTV dose coverage for the old 3D-CRT plans was the most marked among the protocols. The detailed net decreases in the DVH statistics of the CTV after simulating the systematic uncertainties are indicated in Table 5.

The mean DVH of the CTV for the new 3D-CRT plans created on the CT data sets for the IMRT protocol is shown in Fig. 4. The net decreases in the V95, D95, minimum dose, maximum dose, and the mean dose for the IMRT protocol, the new 3D-CRT protocol, and the new 3D-CRT plans created on the CT data sets scanned in the prone position are indicated in Fig. 5. Although the net decreases in the V95, D95, minimum dose, maximum dose, and mean dose became much smaller when the new 3D-CRT plans were created with the patients in the prone position with hip fixation than when created with the patients in the supine

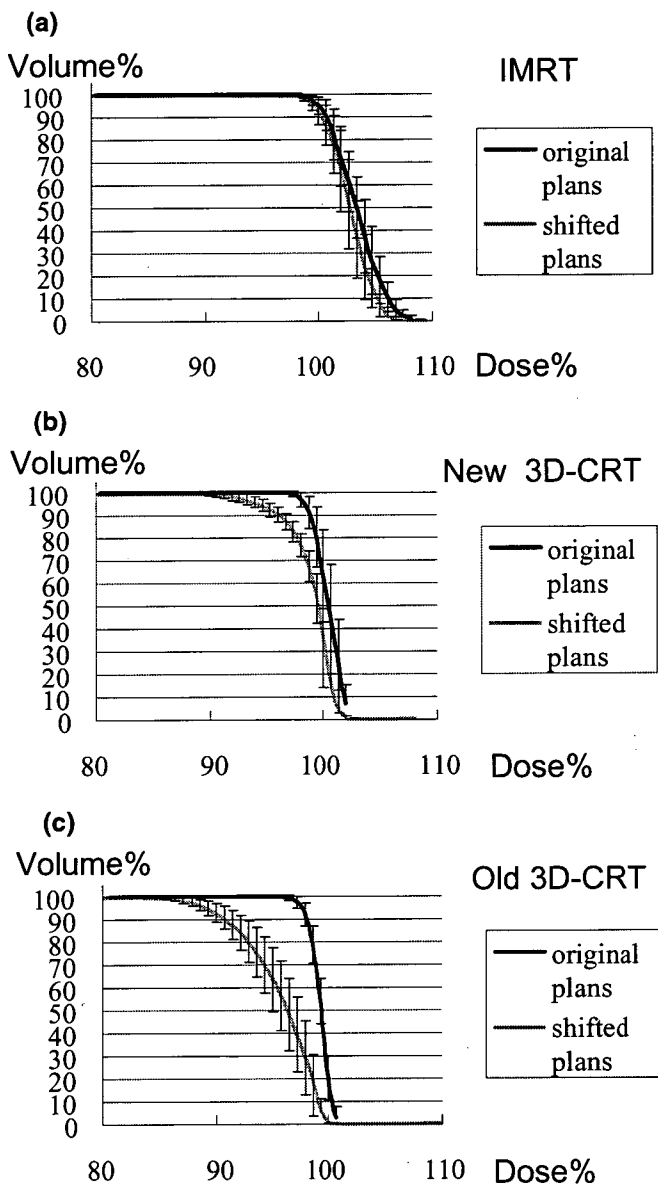


**Fig. 3a-c.** Mean DVH of the CTV before and after taking systematic uncertainties into consideration, for IMRT (a), new 3D-CRT (b), and old 3D-CRT protocols (c). Error bar,  $\pm 1$  SD

**Table 5.** Comparison of the net decreases in the DVH statistics of the CTV for the three protocols after simulation of systematic uncertainties

	IMRT		New 3D-CRT		Old 3D-CRT	
	Net decrease (%)	P value	Net decrease (%)	P value	Net decrease (%)	P value
V95	0	0.4	6.9	0.005	36.7	0.004
D95	0.3	0.02	4.3	0.001	8.1	<0.0001
Min.	2.4	0.1	8.3	0.0001	11.8	<0.0001
Max.	1.7	0.003	1	0.006	1.3	0.003
Mean	0.7	<0.0001	1.5	0.0007	3.7	0.0008

V95, Percent target volume receiving 95% of the prescription dose or higher; D95, percent prescription dose covering 95% of the target volume

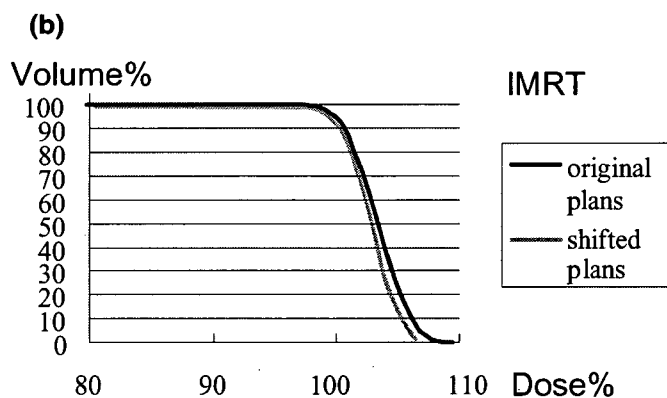
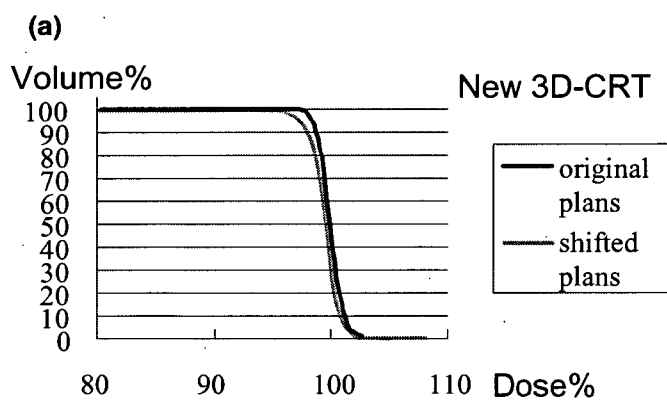


**Fig. 4a,b.** Comparison of the mean DVH of the CTV, for the new 3D-CRT (a) and IMRT plans (b) before and after taking systematic uncertainties into consideration based on the same condition: new 3D-CRT plans were created on the IMRT plan images and the systematic uncertainties of the prone position with hip fixation were simulated for the two protocol plans

position without fixation, the IMRT plans still had some advantages in terms of target coverage.

## Discussion

The ICRU report 50<sup>22</sup> recommends defining a geometrical structure of PTV to compensate for the effect of uncertainties. The magnitude of PTV can predict and project the potential location of the CTV. Margins to create the PTV

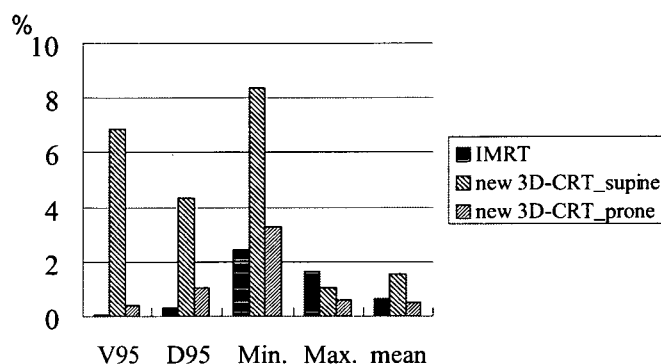


**Fig. 5.** Net decrease in the DVH indexes of the CTV for IMRT, new 3D-CRT\_supine, and new 3D-CRT\_prone plans after taking systematic uncertainties into consideration. *New 3D-CRT\_supine* represents the new 3D-CRT plans simulating the systematic uncertainties in the supine position without using an immobilization device. *New 3D-CRT\_prone* represents the new 3D-CRT plans created based on the IMRT plan images simulating the systematic uncertainties in the prone position with hip fixation

from the CTV (PTV margin) should take into account both setup errors and internal organ motion. However, in most cases, the CTV is often located adjacent to the organs at risk (OARs), which prevents us from using margins large enough to cover all of the uncertainties for most patients. Therefore, adequate margins to compensate for 90%–95% of the uncertainties should be used to create the PTV. More importantly, the magnitude of the adequate margin is also influenced by the method of patient fixation or error reduction strategies. To see whether the defined margins account for the uncertainties, we examined and compared the adequacy of three definitive radiotherapy protocols for localized prostate cancer, in terms of the CTV coverage, by simulating possible large systematic errors with respect to patient setup and internal organ motion.

In the present study, several assumptions were made, based on the previously published literature; we assumed that random errors have a relatively smaller impact on the dose distribution to the prostate,<sup>15-17</sup> while systematic errors are in normal distribution.<sup>4,7,10,20</sup> Because our purpose was to compare planning strategies of three different radiotherapy protocols and to estimate their validity by verifying the tolerability in CTV coverage, we only simulated systematic

errors. To include all the possible systematic uncertainties, it would be necessary to apply nearly  $\pm 3$  SD. However, we carefully chose  $\pm 1.65$  SD of the systematic error as a check-point value for the isocenter shift, which includes 90% (from 5% to 95%) systematic uncertainties along each axis. Therefore, there were in total eight check points (Fig. 1). With these check points, we expected to include most of the possible systematic displacements while excluding very extreme shifts, which is reasonable for comparing the adequacy among different radiotherapy protocols.

Our previous study showed that the dynamic-arc 3D-CRT (new 3D-CRT) could achieve a comparable dose distribution to that achieved with IMRT with respect to the target coverage and rectal sparing in external-beam radiotherapy for localized prostate cancer with a prescription dose of 74 Gy. On the other hand, the old 3D-CRT plan could not reach a qualified dose coverage for the target, based on the current PTV concept, due to the universally smaller portal margins applied.<sup>18</sup> This continuing study shows that when the systematic uncertainties were incorporated into the dose distribution analyses, the difference between the planned and the actually delivered target dose was much larger for the old 3D-CRT plan, and a detectable dose decrease also appeared in the dynamic-arc 3D-CRT plan. However, the IMRT plan still maintained an intended target coverage of the prostate (CTV). Therefore the IMRT protocol is considered to be superior to the dynamic-arc 3D-CRT plan in terms of tolerability against systematic uncertainties.

A big question here is what are the adequate acceptance criteria with respect to the dose decrease from the planned to the actually delivered dose supposing the random factors could be neglected. The answer could not be drawn from the literature. van Herk<sup>17</sup> discussed this point in his review article and analyzed several examples, but the criteria were diverse and could not be uniformly applied: they should be institution-dependent and also treatment-technique-dependent. A general guideline for the target coverage in traditional static dose distribution is reported in ICRU report 50,<sup>22</sup> where the PTV should guarantee that 95% of the prescription dose is delivered to at least 90% of the CTV. Based on this guideline, the actually delivered dose distribution with the old 3D-CRT plans is unacceptable, which means margins applied directly to the CTV and simply defined by jaws/MLCs are universally insufficient to account for systematic uncertainties. However, the difference between the planned and actually delivered dose distribution to the CTV with IMRT plans is nominal, indicating that the margins set successfully compensate for the systematic uncertainties.

There are two main reasons why the ability to account for the systematic uncertainties between our IMRT and the new 3D-CRT protocol plans is different. One is patient position-related and immobilization-related uncertainty values, and the other is the treatment techniques themselves, which define dose conformity to, and the dose gradient from, the PTV. A comparison of the effect of the systematic uncertainties on the new 3D-CRT plans and the IMRT plans based on the same image pool simulating the same values of uncertainties, resulted in the slight supe-

riority of the IMRT protocol to the new 3D-CRT protocol to account for the systematic uncertainties. At the same time, we also noticed that the degree of decrease in dose coverage after simulating the systematic uncertainties for the new 3D-CRT plans was much smaller when the patients were fixed in the prone position and immobilized with hip fixation than when they were treated in the supine position without any fixation devices. This may indicate that if, for our new 3D-CRT protocol, we also immobilize patients in the prone position with hip fixation, as is done with the patients receiving the IMRT protocol, we may get much better actual dose distribution. It has been reported that the prostate movement in the prone position was much larger than that in the supine position if no fixation devices were used, probably because of the effect of respiration.<sup>11</sup> Therefore, it is strongly recommended that we should use a fixation device when treating patients in the prone position.

There were some remarks in the literature that the IMRT was more sensitive to uncertainties than 3D-CRT due to its sharper dose gradients in the peripheral region of the PTV. Our data show that this is not necessarily true. The sensitivity to treatment-related uncertainties strongly depends on the given margins for the PTV and the error reduction strategies applied, as well as the degree of dose fall-off outside the PTV.

One drawback of the present study was that the effect of systematic uncertainties on the doses to the rectum and bladder was not incorporated into the dose distribution analyses of the target. The original planned dose range to the rectum and bladder was large, and rectum filling was diverse; all these factors make the incorporation much more complicated. Therefore, we believe a deformable image registration technique should be incorporated in the treatment planning based on a 4D imaging data set in the future.

In conclusion, differences in the CTV dose among three protocols for definitive external-beam radiotherapy when systematic uncertainties were taken into consideration were evaluated. Our current IMRT protocol, with fixation devices used in the prone position, was considered to successfully compensate for decreased systematic uncertainties, while the old 3D-CRT protocol was inadequate to realize an adequate CTV dose, although the CTV dose was sufficient in terms of the static protocol data. In the future, a 4D dataset-based method for radiotherapy protocol evaluation will be necessary to accurately estimate the actually delivered dose to the targets and organs at risk.

**Acknowledgments** This study was supported in part by a Grant-in-Aid for Scientific Research on Priority Areas Cancer from the Ministry of Education, Culture, Sports, Science and Technology of Japan (No. 17016036), and a Grant-in-Aid for Scientific Research from the Ministry of Education, Culture, Sports, Science and Technology of Japan (No. 16659316 and 17390333).

## References

1. Bijhold J, Lebesque JV, Hart AA, et al. (1992) Maximizing setup accuracy using portal images as applied to a conformal boost technique for prostatic cancer. *Radiother Oncol* 24:261-271

2. Hurkmans CW, Reimeijer P, Lebesque JV, et al. (2001) Setup verification using portal imaging; review of current clinical practice. *Radiother Oncol* 58:105–120
3. Vigneault E, Pouliot J, Laverdiere J, et al. (1997) Electronic portal imaging device detection of radioopaque markers for the evaluation of prostate position during megavoltage irradiation: a clinical study. *Int J Radiat Oncol Biol Phys* 37:205–212
4. Antolak JA, Rosen II, Childress CH, et al. (1998) Prostate target volume variations during a course of radiotherapy. *Int J Radiat Oncol Biol Phys* 42:661–672
5. Beard CJ, Kijewski P, Bussiere M, et al. (1996) Analysis of prostate and seminal vesicle motion: implications for treatment planning. *Int J Radiat Oncol Biol Phys* 34:451–458
6. Lattanzi J, McNeely S, Hanlon A, et al. (1998) Daily CT localization for correcting portal errors in the treatment of prostate cancer. *Int J Radiat Oncol Biol Phys* 41:1079–1086
7. Roeske JC, Forman JD, Mesina CF, et al. (1995) Evaluation of changes in the size and location of the prostate, seminal vesicles, bladder, and rectum during a course of external beam radiation therapy. *Int J Radiat Oncol Biol Phys* 33:1321–1329
8. Stroom JC, Koper PC, Korevaar GA, et al. (1999) Internal organ motion in prostate cancer patients treated in prone and supine treatment position. *Radiother Oncol* 51:237–248
9. Zelefsky MJ, Crean D, Mageras GS, et al. (1999) Quantification and predictors of prostate position variability in 50 patients evaluated with multiple CT scans during conformal radiotherapy. *Radiother Oncol* 50:225–234
10. Balter JM, Sandler HM, Lam K, et al. (1995) Measurement of prostate movement over the course of routine radiotherapy using implanted markers. *Int J Radiat Oncol Biol Phys* 31:113–118
11. Kitamura K, Shirato H, Seppenwoolde Y, et al. (2002) Three-dimensional intrafractional movement of prostate measured during real-time tumor-tracking radiotherapy in supine and prone treatment positions. *Int J Radiat Oncol Biol Phys* 53:1117–1123
12. Wu J, Haycocks T, Alasti H, et al. (2001) Positioning errors and prostate motion during conformal prostate radiotherapy using on-line isocentre setup verification and implanted prostate markers. *Radiother Oncol* 61:127–133
13. Little DJ, Dong L, Levy LB, et al. (2003) Use of portal images and BAT ultrasonography to measure setup error and organ motion for prostate IMRT: implications for treatment margins. *Int J Radiat Oncol Biol Phys* 56:1218–1224
14. Trichter F, Ennis RD (2003) Prostate localization using transabdominal ultrasound imaging. *Int J Radiat Oncol Biol Phys* 56:1225–1233
15. Bortfeld T, Jiang SB, Rietzel E (2004) Effects of motion on the total dose distribution. *Semin Radiat Oncol* 14:41–51
16. Levitt SH, Khan FM (2001) The rush to judgment: does the evidence support the enthusiasm over three-dimensional conformal radiation therapy and dose escalation in the treatment of prostate cancer? *Int J Radiat Oncol Biol Phys* 51:871–879
17. van Herk M (2004) Errors and margins in radiotherapy. *Semin Radiat Oncol* 14:52–64
18. Zhu S, Mizowaki T, Nagata Y, et al. (2005) Comparison of three radiotherapy treatment planning protocols of definitive external-beam radiation for localized prostate cancer. *Int J Clin Oncol* 10:398–404
19. International Commission on Radiation Units and Measurements (1999) ICRU Report 62: prescribing, recording, and reporting photon beam therapy (supplement to ICRU report 50). Oxford University Press, Oxford
20. Rudat V, Schraube P, Oetzel D, et al. (1996) Combined error of patient positioning variability and prostate motion uncertainty in 3D conformal radiotherapy of localized prostate cancer. *Int J Radiat Oncol Biol Phys* 35:1027–1034
21. van't Riet A, Mak AC, Moerland MA, et al. (1997) A conformation number to quantify the degree of conformality in brachytherapy and external beam irradiation: application to the prostate. *Int J Radiat Oncol Biol Phys* 37:731–736
22. International Commission on Radiation Units and Measurements (1993) ICRU Report 50: prescribing, recording, and reporting photon beam therapy. Oxford University Press, Oxford

## INTERINSTITUTIONAL VARIATIONS IN PLANNING FOR STEREOTACTIC BODY RADIATION THERAPY FOR LUNG CANCER

YUKINORI MATSUI, M.D.,\* KENJI TAKAYAMA, M.D.,\* YASUSHI NAGATA, M.D., PH.D.,\*  
ETSUO KUNIEDA, M.D., PH.D.,† KUNHIKO TATEOKA, PH.D.,‡ NAOKI ISHIZUKA, PH.D.,§  
TAKASHI MIZOWAKI, M.D., PH.D.,\* YOSHIKI NORIHISA, M.D.,\* MASATO SAKAMOTO, M.D.,\*  
YUICHIRO NARITA, PH.D.,\* SATOSHI ISHIKURA, M.D., PH.D.,¶ AND MASAHIRO HIRAOKA, M.D., PH.D.,\*

\*Department of Radiation Oncology and Image-applied Therapy, Kyoto University, Kyoto, Japan; †Department of Radiology, Keio University, Tokyo, Japan; ‡Radiation Oncology, Imaging and Diagnosis, Molecular and Organ Regulation, Sapporo Medical University, Graduate School of Medicine, Sapporo, Japan; §Division of Preventive Medicine, Department of Community Health and Medicine, Research Institute, International Medical Center of Japan, Tokyo, Japan; and ¶Radiation Oncology Division, National Cancer Center Hospital East, Kashiwa, Japan

**Purpose:** The aim of this study was to assess interinstitutional variations in planning for stereotactic body radiation therapy (SBRT) for lung cancer before the start of the Japan Clinical Oncology Group (JCOG) 0403 trial.

**Methods and Materials:** Eleven institutions created virtual plans for four cases of solitary lung cancer. The created plans should satisfy the target definitions and the dose constraints for the JCOG 0403 protocol.

**Results:** FOCUS/XiO (CMS) was used in six institutions, Eclipse (Varian) in 3, Cadplan (Varian) in one, and Pinnacle3 (Philips/ADAC) in one. Dose calculation algorithms of Clarkson with effective path length correction and superposition were used in FOCUS/XiO; pencil beam convolution with Batho power law correction was used in Eclipse and Cadplan; and collapsed cone convolution superposition was used in Pinnacle3. For the target volumes, the overall coefficient of variation was 16.6%, and the interinstitutional variations were not significant. For maximal dose, minimal dose, D95, and the homogeneity index of the planning target volume, the interinstitutional variations were significant. The dose calculation algorithm was a significant factor in these variations. No violation of the dose constraints for the protocol was observed.

**Conclusion:** There can be notable interinstitutional variations in planning for SBRT, including both interobserver variations in the estimate of target volumes as well as dose calculation effects related to the use of different dose calculation algorithms. © 2007 Elsevier Inc.

Stereotactic body radiation therapy, Lung cancer, Treatment planning, Interinstitutional variation.

### INTRODUCTION

Promising clinical results of stereotactic body radiation therapy (SBRT) for early-stage lung cancer have been reported by several investigative groups (1–11). However, most of these results were based on data from a single institution, and the treatment protocols differed among institutions. To confirm the

clinical value of SBRT for early-stage lung cancer in multi-institutional settings, the Japan Clinical Oncology Group (JCOG) has planned a multi-institutional trial of SBRT for T1N0M0 lung cancer (the JCOG 0403 protocol).

It was recognized that large interinstitutional variations in the trial would damage its credibility and that such variations should be avoided. We conducted a study of planning

Reprint requests to: Yasushi Nagata, M.D., Ph.D., Department of Radiation Oncology and Image-applied Therapy, Graduate School of Medicine, Kyoto University, 54 Kawahara-cho, Shogoin, Sakyo-ku, Kyoto, 606-8507, Japan. Tel: (+81) 75-751-3418; Fax: (+81) 75-751-3418; E-mail: nag@kuhp.kyoto-u.ac.jp

Presented in part at the 47th Annual Meeting of the American Society for Therapeutic Radiology and Oncology (ASTRO), Denver, CO, October 16–20, 2005.

Supported by Grant-in-Aid No. H18-014 from the Ministry of Health, Labour and Welfare, Japan.

Conflict of interest: none.

**Acknowledgments**—The authors gratefully acknowledge Mr. Daniel Mrozek for editorial assistance. The authors also appreciate the cooperation of the following institutions that have participated

in the Japan Clinical Oncology Group 0403 protocol: Hokkaido University (Sapporo, Japan), Sapporo Medical University (Sapporo, Japan), Tohoku University (Sendai, Japan), Tokyo Metropolitan Komagome Hospital (Tokyo, Japan), Keio University (Tokyo, Japan), Cancer Institute Hospital (Tokyo, Japan), Nihon University (Tokyo, Japan), Tokyo Women's Medical University (Tokyo, Japan), University of Tokyo (Tokyo, Japan), Kitasato University (Sagamihara, Japan), University of Yamanashi (Tamaho, Japan), Kyoto University (Kyoto, Japan), Tenri Hospital (Nara, Japan), Institute of Biomedical Research and Innovation (Kobe, Japan), Hiroshima University (Hiroshima, Japan) and Kyushu University (Fukuoka, Japan).

Received June 29, 2006, and in revised form Dec 8, 2006. Accepted for publication Dec 14, 2006.





Fig. 1. Images of the cases: (a) Case 1, (b) Case 2, (c) Case 3, and (d) Case 4. Each case is a solitary lung tumor. The tumors were T1 in size (within 3 cm) except for that in Case 4. Figure continues on next page.

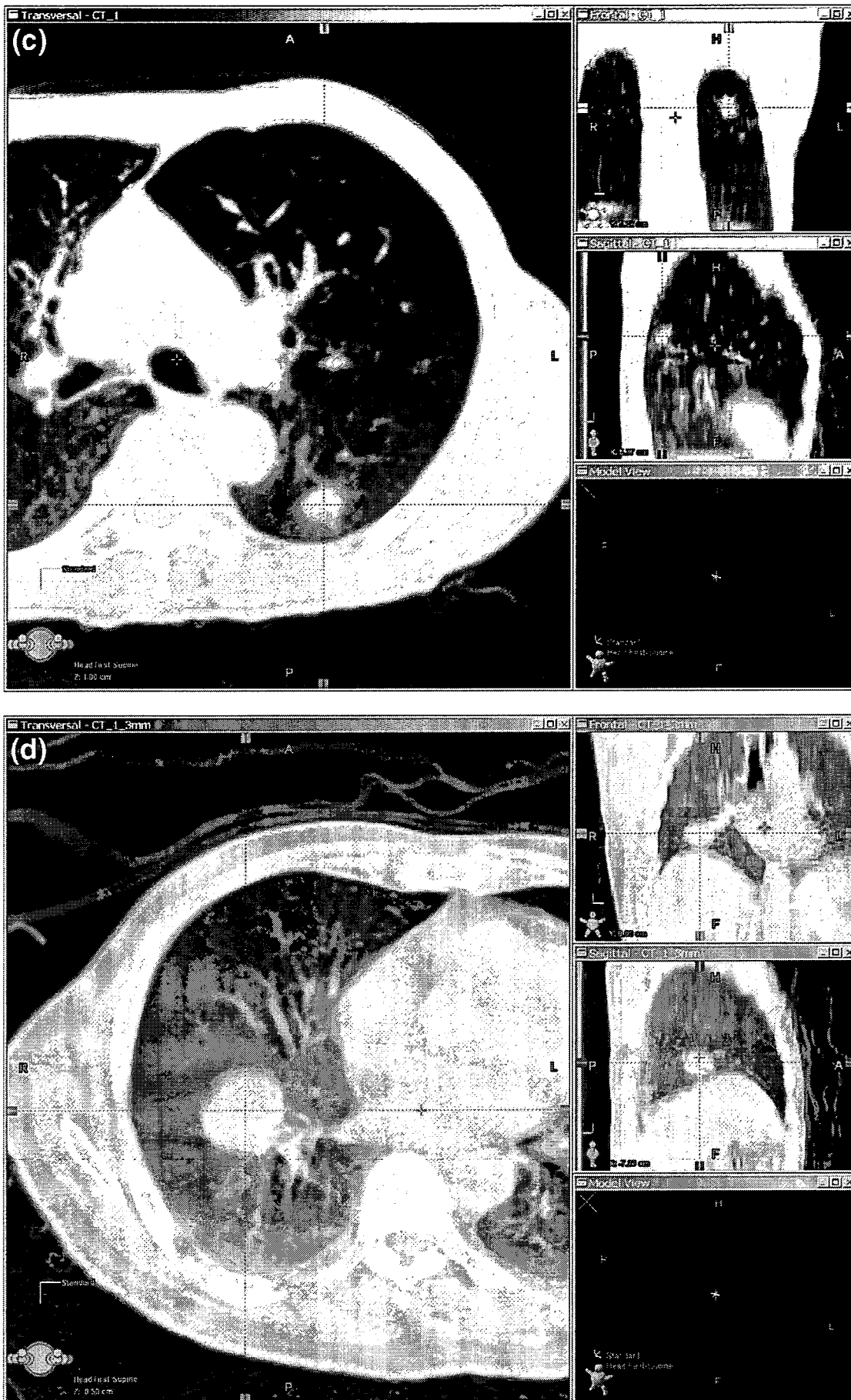


Fig. 1. (Continued)

Table 1. Institutional characteristics

Institution	Beam energy	Irradiation technique	TPS	Calculation algorithm
A	6 MV	Static 6 ports	FOCUS/XiO	CL/SP*
B	10 MV	Mixed 9 groups / Static 10 ports <sup>†</sup>	FOCUS/XiO	CL/SP*
C	6 MV	Static 7 ports	Eclipse	PBC
D	6 MV	Static 3 arcs (total 400 degrees) <sup>‡</sup>	FOCUS/XiO	SP
E	6 MV	Dynamic 10 arcs (total 1,600 degrees)	FOCUS/XiO	SP
F	6 MV	Static 8 ports	Pinnacle3	CC
G	6 MV	Static 5–10 ports	Eclipse	PBC
H	6, 10 MV	Static 7–8 ports	Eclipse	PBC
I	6 MV	Static 8 ports	Cadplan	PBC
J	4 MV	Static 6 ports	FOCUS/XiO	SP
K	6 MV	Static 10 ports	FOCUS/XiO	CL

*Abbreviations:* CC = collapsed cone convolution superposition; CL = Clarkson with effective path length correction; PBC = pencil beam convolution with Batho power law correction; SP = superposition; TPS = treatment planning system;

\* Institutions A and B changed their algorithm from CL to SP between the series.

<sup>†</sup> Institution B changed its technique from a mixed style of arcs and static ports to static ports only between the series.

<sup>‡</sup> No multileaf collimator was implemented in institution D.

Table 2. Target volumes delineated by 11 institutions on 4 cases

	Target volumes (cc)			
	Case 1	Case 2	Case 3	Case 4
A	9.0	11.0	6.0	34.0
B	4.8	8.2	5.1	36.0
C	5.7	10.7	6.2	35.4
D	8.6	14.1	3.1	28.5
E	7.4	10.7	7.8	33.4
F	6.9	9.5	4.2	28.7
G	7.5	12.8	7.4	29.2
H	6.6	13.1	5.5	34.8
I	7.5	14.2	6.7	38.9
J	8.0	10.0	4.0	30.0
K	9.0	12.0	10.0	38.0
Mean	7.4	11.5	6.0	33.4
SD	1.3	1.9	2.0	3.7
CV	17.9%	16.8%	32.7%	11.2%

*Abbreviations:* CV = coefficient of variation; SD = standard deviation.

for SBRT for lung cancer before the start of the JCOG 0403 protocol to assess interinstitutional variations in treatment planning.

## METHODS AND MATERIALS

This study was performed in two series. In the first series in March 2004, seven institutions (A–G) were asked to create virtual plans for two cases (Cases 1 and 2; Figs. 1a and 1b). In the second series in June 2004, two additional cases (Cases 3 and 4; Figs. 1c and 1d) were added, and institutions A to G made plans for them. At the same time, four institutions (H–K) joined the study and created plans for Cases 1 to 4. In total, the 11 institutions created virtual plans for the four cases.

### Cases

Each case was a solitary lung cancer of T1 size (within 3 cm), except for Case 4 (3.6 cm). Computed tomographic (CT) images of Cases 1 and 2 were acquired under breath-holding with 2-mm-thick slices around the tumor and 5-mm-thick slices elsewhere. The CT images of Cases 3 and 4 were acquired under free-breathing with 3-mm-thick slices around the tumor and 5-mm-thick slices elsewhere using the “long-scan-time” technique, which can visualize a major part of the trajectory of tumor movement by scanning each slice for a long time (12). The images were transferred to the participants in a Digital Imaging and Communications in Medicine–formatted CD-ROM.

### Treatment planning

Radiation oncologists who were responsible for SBRT planning in each institution planned for the cases in accordance with the JCOG

Table 3. Dose-volumetric data of the planning target volumes (PTVs)

	Case 1	Case 2	Case 3	Case 4
PTVmax (Gy)	49.2 ± 0.7	49.1 ± 0.7	48.9 ± 0.9	49.4 ± 0.9
PTVmin (Gy)	41.4 ± 4.8	42.5 ± 3.5	42.9 ± 2.8	41.0 ± 3.9
D95 (Gy)	44.3 ± 3.3	45.0 ± 2.3	43.9 ± 3.6	43.3 ± 4.3
HI	1.20 ± 0.16	1.16 ± 0.09	1.14 ± 0.06	1.22 ± 0.14
CI	2.04 ± 0.55	1.80 ± 0.32	2.02 ± 0.47	1.75 ± 0.13

*Abbreviations:* CI = conformity index; HI = homogeneity index.

Data are shown as mean ± SD.

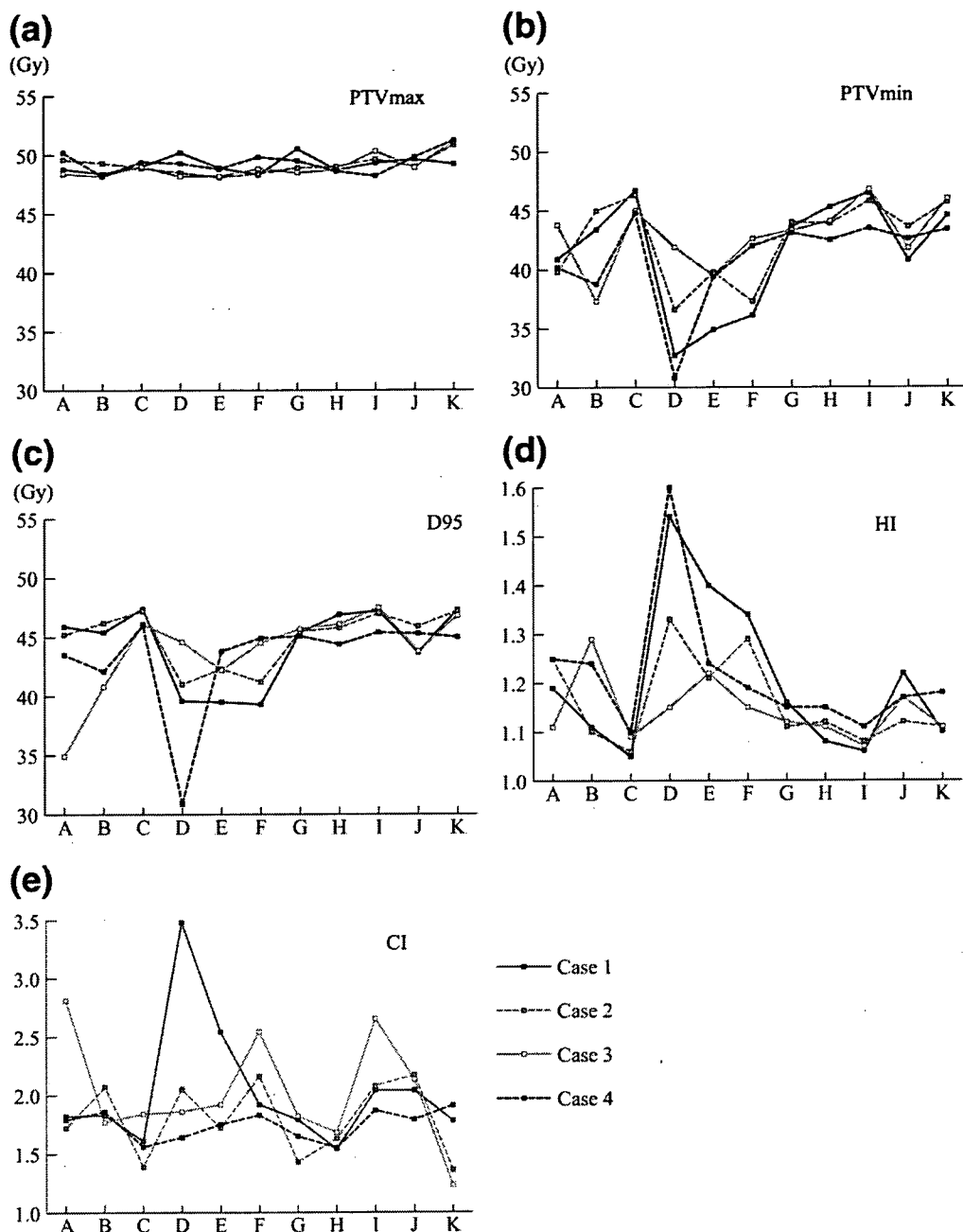


Fig. 2. Variations in the dose–volumetric data of planning target volume (PTV); (a) PTVmax, (b) PTVmin, (c) D95, (d) Homogeneity Index (HI), and (e) conformity index (CI). Lines join points of the same cases. The interinstitutional variations were significant in PTVmax ( $p = 0.014$ ), PTVmin ( $p < 0.001$ ), D95 ( $p = 0.007$ ) and HI ( $p < 0.001$ ). Significant differences were observed between institution K and institutions B, E, F, and H in PTVmax; between institution D and institutions C, G, H, I, J, and K, between institution E and institutions C, I, and K, and between institution F and institutions C and I in PTVmin; between institution D and institutions C, I and K in D95; and between institution D and institutions A, B, C, G, H, I, J, and K in HI. The maximal differences in mean levels of institution were 2.1 Gy in PTVmax (between institutions E and K), 10.2 Gy in PTVmin (between institutions C and D), 7.8 Gy in D95 (between institutions D and K), and 0.33 in HI (between institutions D and I).

0403 protocol (see Appendix). The planning included the following procedures: delineation of targets and organs at risk (OARs); selection of beam energy; arrangement of irradiation beams; and dose calculation using their treatment planning systems. In Cases 1 and 2, gross tumor volumes (GTVs) were contoured on the images, and clinical target volumes (CTVs) were set to be identical to the GTVs. Respiratory motion was assumed to be negligible in this virtual

planning, so internal target volumes (ITVs) were identical to the GTVs. In Cases 3 and 4, ITVs were directly delineated on the long-scan-time CT images. In all cases, planning target volumes (PTVs) were created by adding 5-mm margins to the ITVs in all directions. Planning OAR volumes (PRVs) were defined for the heart in Case 2, for the aorta in Case 3, and for the spinal cord and the lung in all cases. The margin between PRVs and OARs was 5 mm except